

Supplementary Information

Repurposing *de novo* designed entities reveals phosphodiesterase 3B and cathepsin L modulators

Tiago Rodrigues,^a Yen-Chu Lin,^b Markus Hartenfeller,^{a,b} Steffen Renner,^b
Yi Fan Lim^a and Gisbert Schneider^a

^a Swiss Federal Institute of Technology (ETH), Department of Chemistry and Applied
Biosciences, Vladimir-Prelog-Weg 4, 8093 Zürich, Switzerland

^b Novartis Pharma AG, Postfach, 4002 Basel, Switzerland

Table of contents

1. Computational methods.....	S2
1.1 <i>De novo</i> design.....	S2
1.2 Target and affinity prediction.....	S4
2. Chemistry.....	S4
2.1 General considerations.....	S4
2.2 Syntheses.....	S5
2.3 Dynamic light scattering.....	S6
3. Biology.....	S7
3.1 Protease and PDE assays.....	S7
3.2 <i>In vitro</i> MCF7 cell growth inhibition.....	S8
4. Supplementary data.....	S9
4.1 NMR.....	S9
4.2 Dynamic light scattering.....	S15
4.3 Predicted <i>pAffinity</i>	S19
4.4 Targets predicted with SEA and SPiDER for compounds 1-6	S20
4.5 Biochemical data.....	S26
5. References.....	S27

1. Computational methods

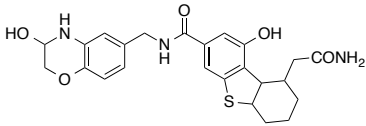
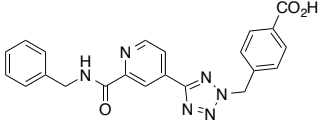
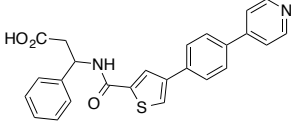
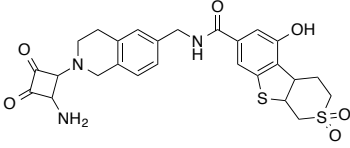
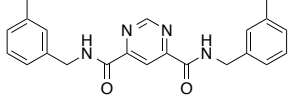
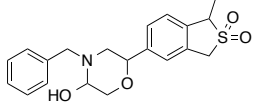
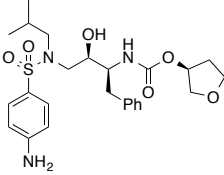
1.1 De novo design

*libDOGS*¹ is an extension of the DOGS software,² optimized for the design of chemical libraries (compound series sharing a substantial part of their molecular structure and strategy for synthesis) rather than singular compounds. Despite this novel aspect *libDOGS* inherited key features from the original DOGS software: 58 standard reaction types have been collected in collaboration with medicinal chemists experienced in the design of chemical libraries. Together with ~26,000 chemical building blocks readily purchasable from commercial suppliers, these chemical reactions define the search space of the de novo design process. *libDOGS* follows a two-step approach, in which the first step is supposed to suggest a chemical scaffolds representing the basis of the chemical series designed in step 2. The selection of the scaffold is semi-automated process: the tool presents the expert user with a subset of scaffolds that can be designed by *libDOGS*. These scaffolds are pre-selected automatically by the software based on scores that measures chemical similarity against ring systems present in the reference ligands (reference scaffolds). The second step of *libDOGS* is a virtual enumeration of chemical libraries based on the scaffold(s) selected after step 1, similar to the greedy design process described for DOGS. The user can chose from various scoring functions to guide the in silico design process (e.g. distance calculation based on different structural fingerprints or a combined overlap of molecular shape and pharmacophore features).

In the example of the MMP project the phenyldihydropyridazinone scaffold was selected as the basis for synthesis of a chemical library of potential MMP modulators after manual inspection of the scaffolds suggested by the software tool. Evolving chemical libraries were scored in step 2 based on average chemical similarity to the reference compounds based on circular substructure fingerprints.

Template structures (Table S1) were standardized using the “wash”, “protonate”, and “add hydrogens” options in MOE 2012.10 (Molecular Operating Environment; The Chemical Computing Group, Montreal, Canada). The software DOGS was run on an eight-core MacPro (OS X 10.6.8) computer with the options $\alpha = 0.1-0.9$ and 200 start fragments, as described previously.² Similarity between the designs and the template was computed using the ISOAK graph kernel method on reduced graph representations.^{2, 3}

Table S1. Template structures used for computational *de novo* design.

Compound	Template structure	Functional activity
S1		MMP-8 inhibitor
S2		MMP-13 inhibitor
S3		MMP-12 inhibitor
S4		MMP-8 inhibitor
S5		MMP-13 inhibitor
S6		MMP-12 inhibitor
Amprenavir		HIV-1 protease inhibitor

1.2 Target and affinity prediction

For training the Gaussian process models we used the ChEMBL database as described previously.^{4,5} Briefly, we generated prediction models for protein targets with more than 200 annotated human bioactivities. All activity end-points were standardized to $pAffinity = -\log_{10}(\text{activity})$. The final affinity data set consisted of 209,293 compounds with 431,313 bioactivities for 469 human targets. Post-processing was conducted using Python (<http://www.python.org>) and Knime v.2.6.0 (Konstanz University, Konstanz, Germany). Molecular structures were standardized using the “wash” function in MOE 2012.10 (The Chemical Computing Group Inc., Montreal, Canada). Two different molecular descriptors were calculated for each compound: (i) topological pharmacophores (CATS2, 0–9 bonds, type-sensitive scaling),⁶ and (ii) topological circular substructure fingerprints (Morgan fingerprint, $radius = 2$, 2048 bit, from RDKit: <http://www.rdkit.org>). Predictive models were implemented using Matlab R2012b (The MathWorks Inc., Natick, USA) and the GPML toolbox v3.1 (<http://www.gaussianprocess.org>).

2. Chemistry

2.1 General considerations

Starting materials and solvents were purchased from Sigma-Aldrich, Fluka, Chembridge, Maybridge or ABCR and were used without further purification. The key tetrahydropyridazin-3-one building block for purchased from Enamine (Monmouth Jct., NJ, USA) and NID-1 was purchased from Merck Millipore, Germany. Syntheses were performed on a Radleys Tech Carousel with 12 reaction stations or on a Biotage Initiator microwave reactor. Melting points (mp) were recorded on a Büchi M560 apparatus and are uncorrected. Proton and carbon nuclear magnetic resonance (¹H and ¹³C NMR) spectra were recorded on a Bruker Avance 400 (400 and 100 MHz, respectively). All chemical shifts are quoted on the δ scale in ppm using residual solvent peaks as the internal standard. Coupling constants (*J*) are reported in Hz with the following splitting abbreviations: s = singlet, d = doublet, t = triplet, m = multiplet. Analytical LC-MS was carried out in a Shimadzu LC-MS2020 system, equipped with a Nucleodur C₁₈ HTec column, under an appropriate gradient of acetonitrile:H₂O (+0.1% formic acid in each solvent), and a total flow rate of 0.5 mL/min. Alternatively, LC-MS analyses were conducted under identical experimental conditions on a VWR-Hitachi LaChrom Elite HPLC coupled to an Advion CMS system. High-resolution mass spectrometry (HRMS) analyses were performed on a Bruker Daltonics maXis ESI-QTOF device. Mass spectrometry analyses were operated in positive-ion mode with ESI. Nominal and exact *m/z* values are reported in Daltons. All compounds present purities $\geq 95\%$ based on LC-UV/Vis analysis.

2.2 Syntheses

General procedure for amide bond formation.

Carboxylic acid (1.0 molar eq.), EDCI (1.25 molar eq.), HOBt (1.65 molar eq.) and amine (0.85 molar eq.) were dissolved in dry CH₂Cl₂ (20 mL/mmol carboxylic acid) and DMF (0.5 mL/mmol carboxylic acid). The reaction mixture was stirred at room temperature for 48 h. The solvent was evaporated under reduced pressure and the crude product purified via preparative HPLC (Eluent A: ACN+0.1% formic acid; Eluent B: H₂O+0.1% formic acid) with a 30-95% ACN gradient, run over 16 minutes.

3-(Benzo[*d*][1,3]dioxol-5-yl)-*N*-(4-(6-oxo-1,4,5,6-tetrahydropyridazin-3-yl)phenyl)propanamide (1)

White powder; 75%; mp = 222-223 °C. ¹H NMR (DMSO-*d*₆, 400.13 MHz): δ 2.43 (2H, m, CH₂), 2.59 (2H, m, CH₂), 2.82-2.94 (4H, m, 2CH₂), 5.96 (2H, s, CH₂), 6.71 (1H, d, *J* = 6.4 Hz, Ar-H), 6.83 (2H, m, Ar-H), 7.63-7.71 (4H, m, Ar-H), 10.04 (1H, s, NH), 10.85 (1H, s, NH). ¹³C NMR (DMSO-*d*₆, 100.61 MHz): δ 21.68, 25.99, 30.44, 38.26, 100.59, 108.05, 108.69, 118.60, 121.00, 126.22, 130.46, 134.88, 140.12, 145.33, 147.12, 149.03, 166.92, 170.55. HRMS-ESI calc. (C₂₀H₁₉N₃O₄+H⁺): 366.1448 Da, found: 366.1451 Da.

***N*-(4-(6-Oxo-1,4,5,6-tetrahydropyridazin-3-yl)phenyl)pyrazine-2-carboxamide (2)** Grey powder; 22%; mp > 250 °C. ¹H NMR (DMSO-*d*₆, 400.13 MHz): δ 2.45 (2H, t, *J* = 8.0 Hz, CH₂), 2.96 (2H, t, *J* = 8.0 Hz, CH₂), 7.77 (2H, d, *J* = 8.4 Hz, Ar-H), 7.99 (2H, d, *J* = 8.4 Hz, Ar-H), 8.83 (1H, s, Ar-H), 8.94 (1H, s, Ar-H), 9.31 (1H, s, Ar-H), 10.86-10.89 (2H, m, NH). ¹³C NMR (DMSO-*d*₆, 100.61 MHz): δ 21.71, 25.98, 120.15, 126.13, 131.65, 139.07, 143.22, 144.08, 144.95, 147.74, 148.96, 161.82, 166.94. HRMS-ESI calc. (C₁₅H₁₃N₅O₂+H⁺): 296.1142 Da, found: 296.1147 Da.

***N*-(4-(6-Oxo-1,4,5,6-tetrahydropyridazin-3-yl)phenyl)acetamide (3)** White powder; 39%; mp > 250 °C. ¹H NMR (DMSO-*d*₆, 400.13 MHz): δ 2.06 (3H, s, CH₃), 2.43 (2H, t, *J* = 8.0 Hz, CH₂), 2.91 (2H, t, *J* = 8.0 Hz, CH₂), 7.63 (2H, d, *J* = 8.8 Hz, Ar-H), 7.70 (2H, d, *J* = 8.8 Hz, Ar-H), 10.08 (1H, s, NH), 10.84 (1H, s, NH). ¹³C NMR (DMSO-*d*₆, 100.61 MHz): δ 21.67, 24.04, 25.99, 118.50, 126.20, 130.41, 140.24, 149.04, 166.93, 168.46. HRMS-ESI calc. (C₁₂H₁₃N₃O₂+H⁺): 232.1081 Da, found: 232.1079 Da.

***N*-(4-(6-Oxo-1,4,5,6-tetrahydropyridazin-3-yl)phenyl)-2-(pyridin-3-yl)acetamide (4)** Grey powder; 21%; mp = 217-218 °C. ¹H NMR (DMSO-*d*₆, 400.13 MHz): δ 2.42 (2H, t, *J* = 8.0 Hz, CH₂), 2.91 (2H, t, *J* = 8.0 Hz, CH₂), 3.73 (2H, s, CH₂), 7.37 (1H, m, Ar-H), 7.64-7.77 (5H, m, Ar-H), 8.46 (1H, m, Ar-H), 8.48 (1H, m, Ar-H), 10.39 (1H, s, NH), 10.85 (1H, s, NH). ¹³C NMR (DMSO-*d*₆, 100.61 MHz): δ 21.67, 25.97, 40.12, 118.75, 123.38, 126.26, 130.76, 131.45, 136.82, 139.95, 147.77, 148.96, 150.16, 166.92, 168.68. HRMS-ESI calc. (C₁₇H₁₆N₄O₂+H⁺): 309.1346 Da, found: 309.1346 Da.

General procedure for Mitsunobu ester bond formation.

Z-L-Phenylalanine (1 molar eq.) and (*R*)- or (*S*)-tetrahydrofuran-3-ol (1 molar eq.) were dissolved in dry THF (10 mL/mmol). Triphenylphosphine (1.25 molar eq.) and DEAD (1 molar eq.) were added, and the mixture heated for 30 minutes at 50 °C under microwaves. The crude mixture was purified from preparative HPLC, under a 50-75% gradient of H₂O : acetonitrile + 0.1% formic acid run over 16 minutes.

(*S*)-Tetrahydrofuran-3-yl ((benzyloxy)carbonyl)-L-phenylalaninate (5) Transparent oil, 90%. ¹H NMR (CDCl₃, 400.13 MHz): δ 1.84 (1H, m, CH), 2.11 (1H, m, CH), 3.22 (2H, d, *J* = 6.4 Hz, CH₂), 3.76-3.92 (4H, m, CH₂), 4.60 (1H, m, CH), 5.12 (2H, s, CH₂), 5.31 (2H, m, CH + NH), 7.15 (2H, d, *J* = 7.6 Hz, Ar-H), 7.27-7.40 (8H, m, Ar-H). ¹³C NMR (CDCl₃, 100.61 MHz): δ 32.56, 38.31, 54.88, 66.91, 67.11, 72.80, 75.91, 127.25, 128.16, 128.27, 128.56, 128.65, 129.29, 135.57, 136.10, 155.70, 171.40. HRMS-ESI calc. (C₂₁H₂₃NO₅+H⁺): 370.1649 Da, found: 370.1645 Da.

(*R*)-Tetrahydrofuran-3-yl ((benzyloxy)carbonyl)-L-phenylalaninate (6) Transparent oil, 84%, ¹H NMR (CDCl₃, 400.13 MHz): δ 1.97 (1H, m, CH), 2.17 (1H, m, CH), 3.15 (2H, d, *J* = 5.6 Hz, CH₂), 3.70 (1H, d, *J* = 10.4 Hz, CH), 3.83-3.88 (3H, m, CH₂+CH), 4.66 (1H, m, CH), 5.13 (2H, s, CH₂), 5.21-5.40 (2H, m, CH + NH), 7.15 (2H, d, *J* = 8.0 Hz, Ar-H), 7.25-7.40 (8H, m, Ar-H). ¹³C NMR (CDCl₃, 100.61 MHz): δ 32.67, 38.23, 54.82, 66.92, 67.03, 72.69, 76.11, 127.23, 128.13, 128.24, 128.56, 128.64, 129.33, 135.57, 136.22, 155.65, 171.33. HRMS-ESI calc. (C₂₁H₂₃NO₅+H⁺): 370.1649 Da, found: 370.1649 Da.

2.3 Dynamic light scattering

Particle size distributions were measured at a wavelength of 660 nm and a scattering angle of 90°, with linear spacing of the correlation time in a Brookhaven digital auto-correlator, and analyzed the data with a digital autocorrelation software (Brookhaven Instruments Corporation, New York, USA). The mean and standard deviation of the particle size distribution were calculated by assuming a lognormal distribution of the intensity-weighted distribution. Stock solution were prepared in dimethylsulfoxide and diluted sequentially in water.

3. Biology

3.1 Protease and PDE assays

Protease and PDE assays were performed on a fee-or-service basis. Compounds were tested at Reaction Biology Corporation (Malvern, PA, USA), using FRET assays.

Matrix metalloproteinase-2, -3, -8, -12, -13. The required enzyme and substrate (5-FAM/QXLTM FRET peptide) were prepared in freshly prepared reaction buffer (50 mM HEPES pH 7.5, 10 mM CaCl₂, 0.01% Brij-35, 0.1 mg/mL BSA, 1% DMSO). The enzyme and compounds were delivered into the reaction well. After 10-15 minutes of incubation, the substrate (5 μM) was delivered to initiate the reaction. The enzyme activities were monitored (Ex/Em 485/520) every 5 minutes as a time-course measurement of the increase in fluorescence signal from the fluorescently-labeled peptide substrate for 120 minutes at room temperature.

HIV-1 protease. The required enzyme and substrate (50X HIV-1 protease substrate EDANS/DABCYL FRET peptide (Anaspec SensoLyte® 490 HIV-1 Protease Assay Kit Cat# 71127, Component A. Final concentration in assay = 1X HIV-1 protease substrate diluted in reaction buffer) were prepared in freshly prepared reaction buffer (2X assay buffer (Anaspec SensoLyte® 490 HIV-1 Protease Assay Kit Cat# 71127, Component D), Store at -20 °C. Add 1% DMSO and 1 mM DDT in buffer before use). The enzyme and compounds were delivered into the reaction well. The substrate was delivered to initiate the reaction. The enzyme activities were monitored (Ex/Em 340/490) as a time-course measurement of the increase in fluorescence signal from the fluorescently-labeled peptide substrate for 120 minutes at room temperature.

Cathepsin L and S. The required enzyme (Enzo, Cat# BML-SE201-0025 for cathepsin L BML-SE453-0010 for cathepsin S) and substrate (Z-FR-AMC (Biomol), 10 μM in reaction well) were prepared in freshly prepared reaction buffer (400 mM Sodium acetate pH 5.5, 4 mM EDTA, 8 mM DTT for cathepsin L and 75 mM Tris pH 7.0, 0.005% Brij35, 3 mM DTT, 4 mM EDTA for cathepsin S). The enzyme and compounds were delivered into the reaction well. The substrate was delivered to initiate the reaction. The enzyme activities were monitored (Ex/Em 355/460) as a time-course measurement of the increase in fluorescence signal from the fluorescently-labeled peptide substrate for 120 minutes at room temperature.

Functional phosphodiesterase 3B (Ref 2705), 10A2 (Ref 2357), 11A4 (Ref 2358), 2A1 (Ref 2426), 3A (Ref 2432), 4A1A (Ref 2342), 4B1 (Ref 2413) and 7A (Ref 2351) activity was tested in a cell-based assay at Cerep (Celle l'Evescault, France), following the procedure described by Bender *et al.*⁷

Table S2. Assay conditions for PDE assays.

Source	Substrate	Measured component	Incubation	Detection method
Human Sf9 cells	cAMP (40 nM)	Residual cAMP	30 min, r.t.	HTRF

3.2 *In vitro* MCF7 cell growth inhibition

The cytotoxic effect of the compounds was evaluated using the MTT assay.⁸ MCF-7 (DMEM with 10% FBS, 1% antibiotic, 1% glutamine), in its complete medium were seeded in 96-well cell culture plates at a density of 10^4 cells per well, and allowed to attach overnight at 37°C. Then, the cells were incubated with different compound concentrations for 24 h and the medium-containing compound was removed. Medium containing 3-(4,5-dimethylthiazol-2-yl)-2,5-diphenyltetrazolium bromide (MTT, 0.5 mg/ml) (ABCR, Germany) was then added to cells and removed after 1 h of incubation. Dimethyl sulfoxide (DMSO, Sigma-Aldrich, U.S.A) was added to dissolve the purple formazan that was reduced from MTT by mitochondria reductase of living cells, and the absorbance was measured at 540 nm.

4. Supplementary data

4.1 NMR

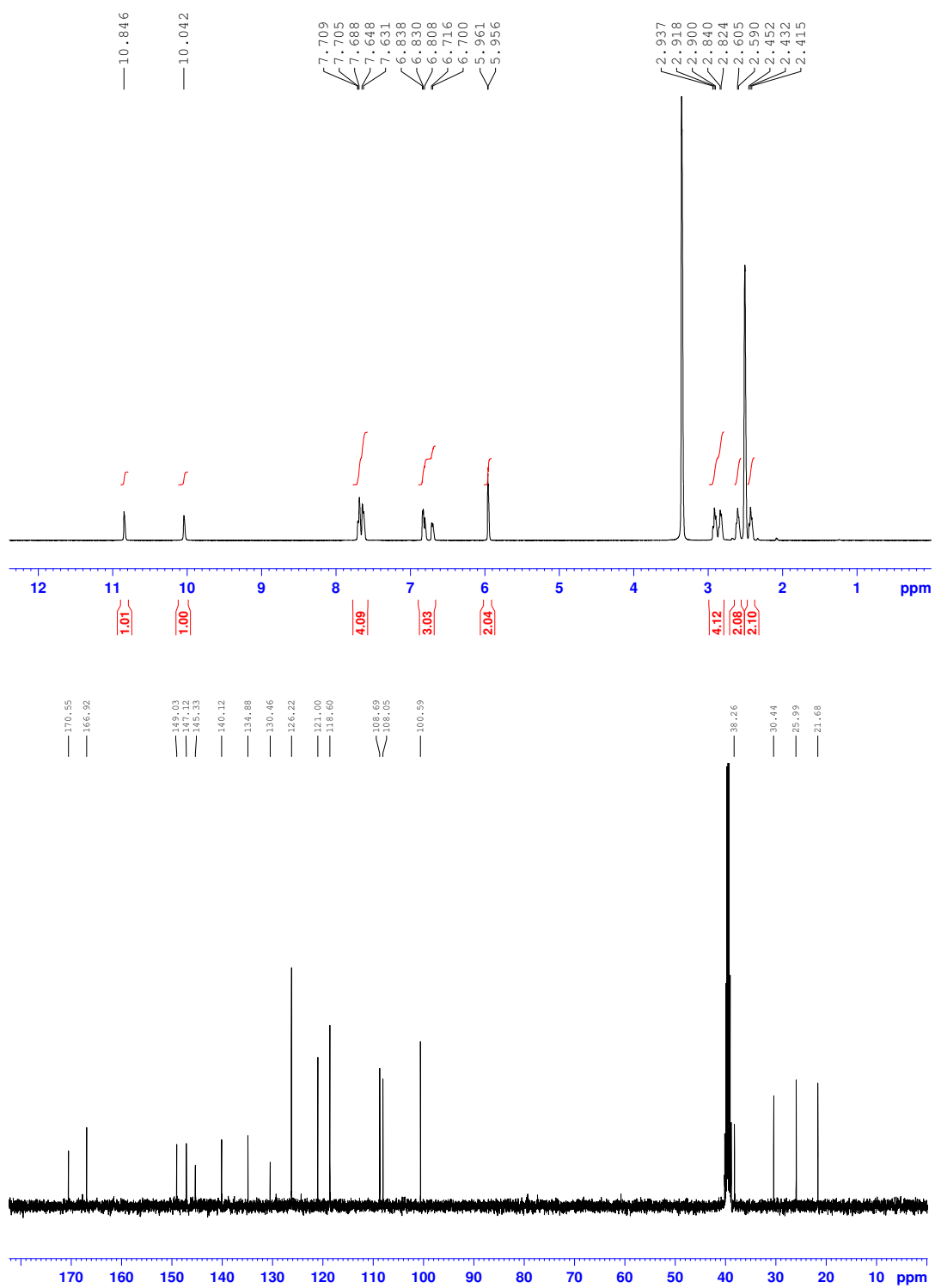


Fig. S1 NMR data of compound 1.

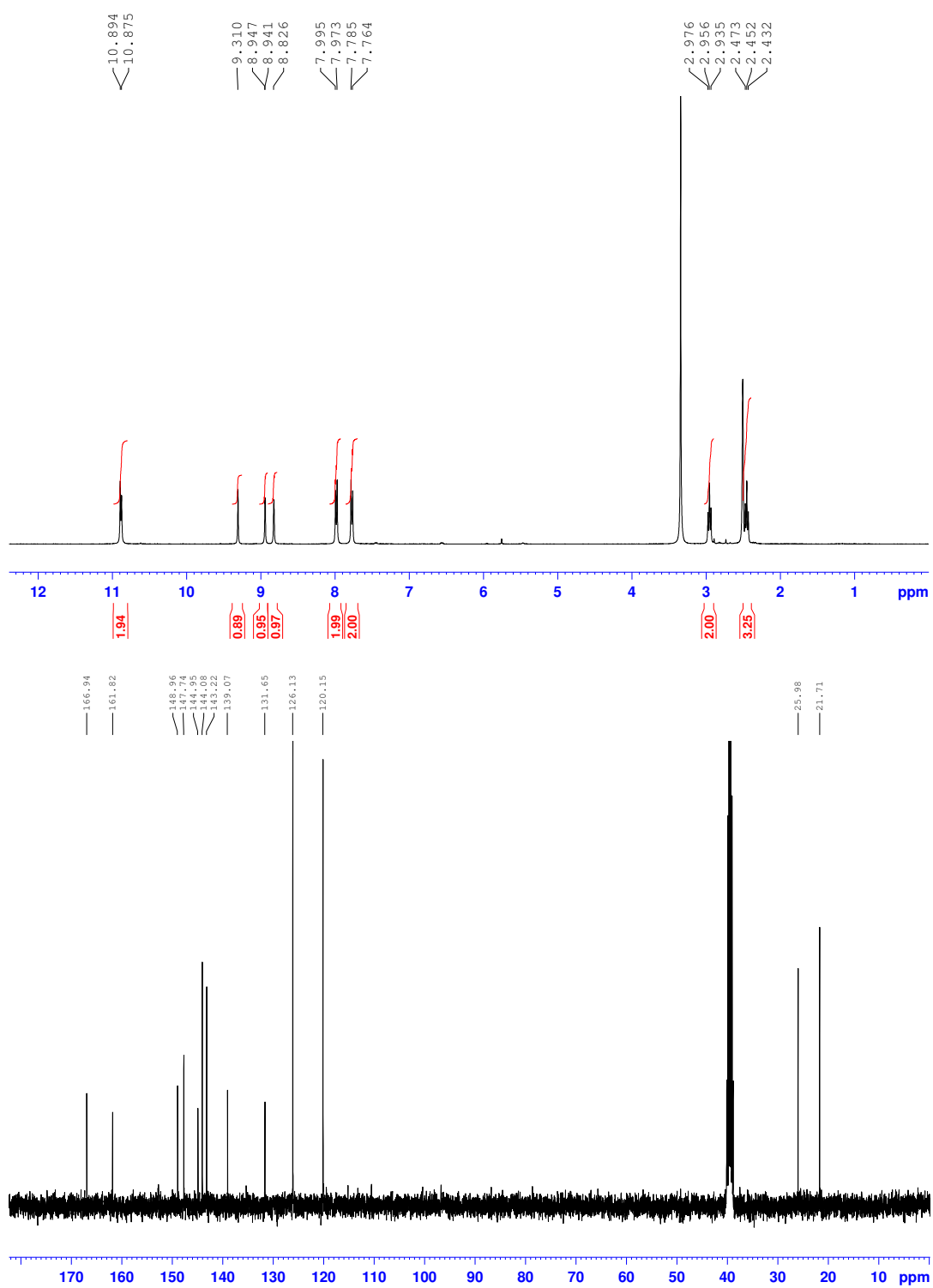


Fig. S2 NMR data of compound 2.

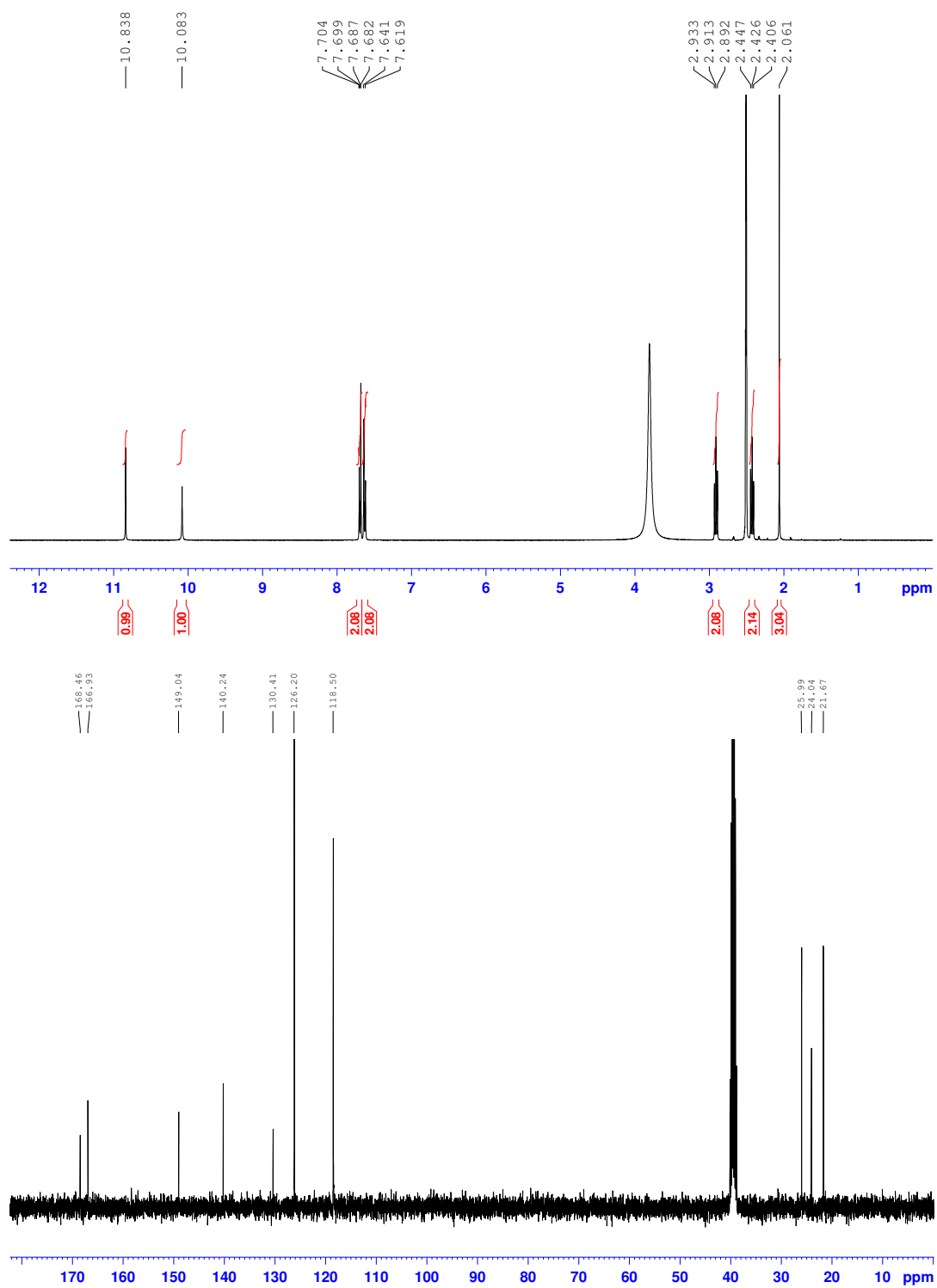


Fig. S3 NMR data of compound 3.

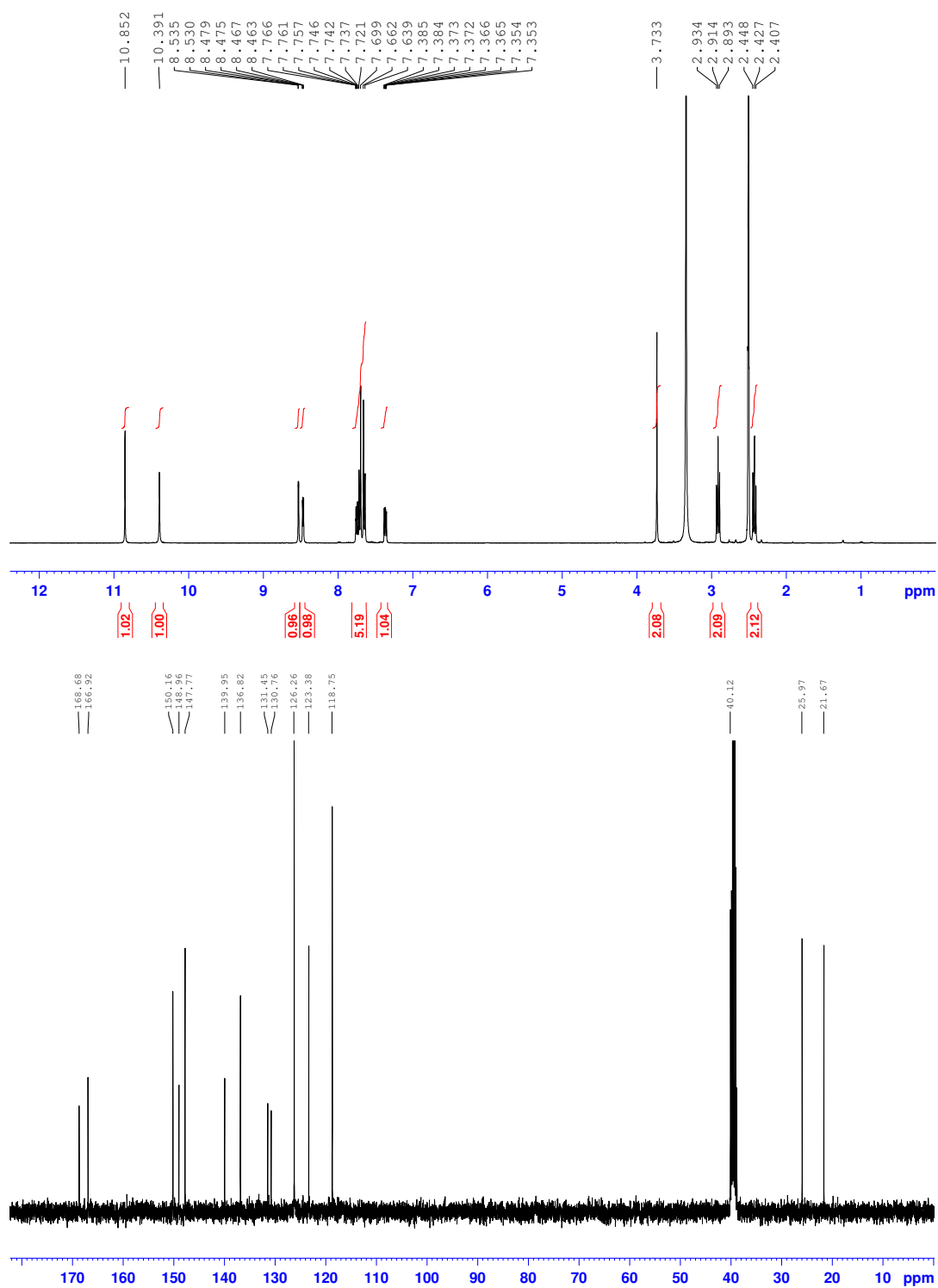


Fig. S4 NMR data of compound 4.

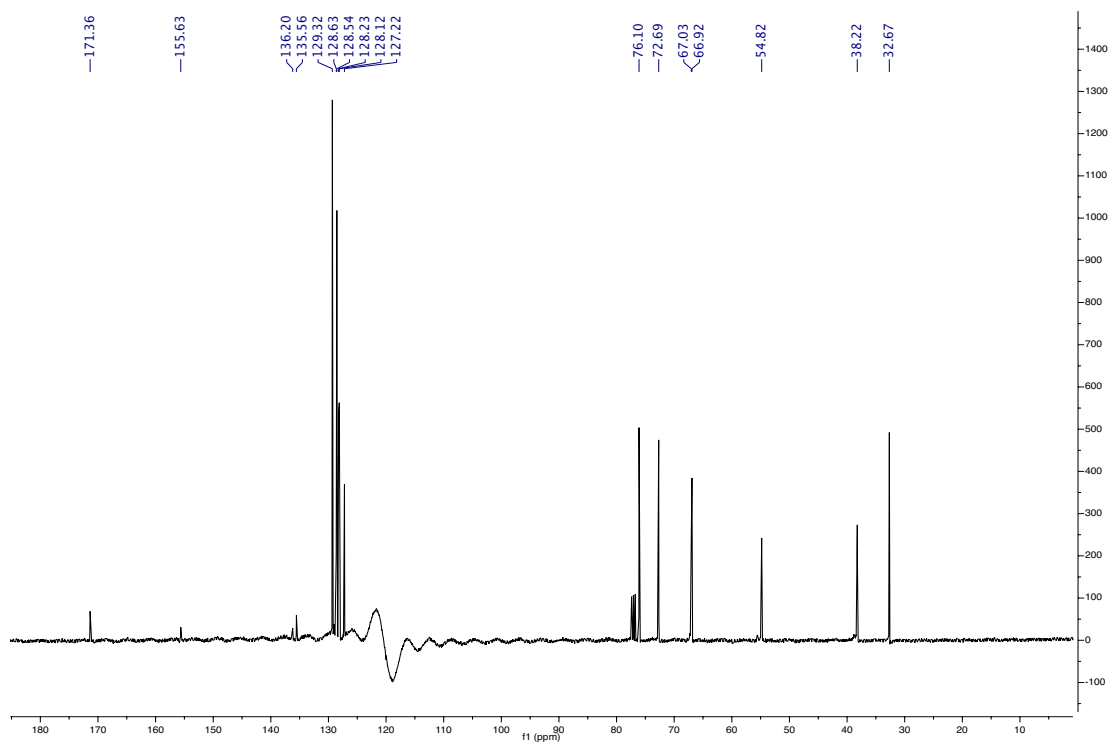
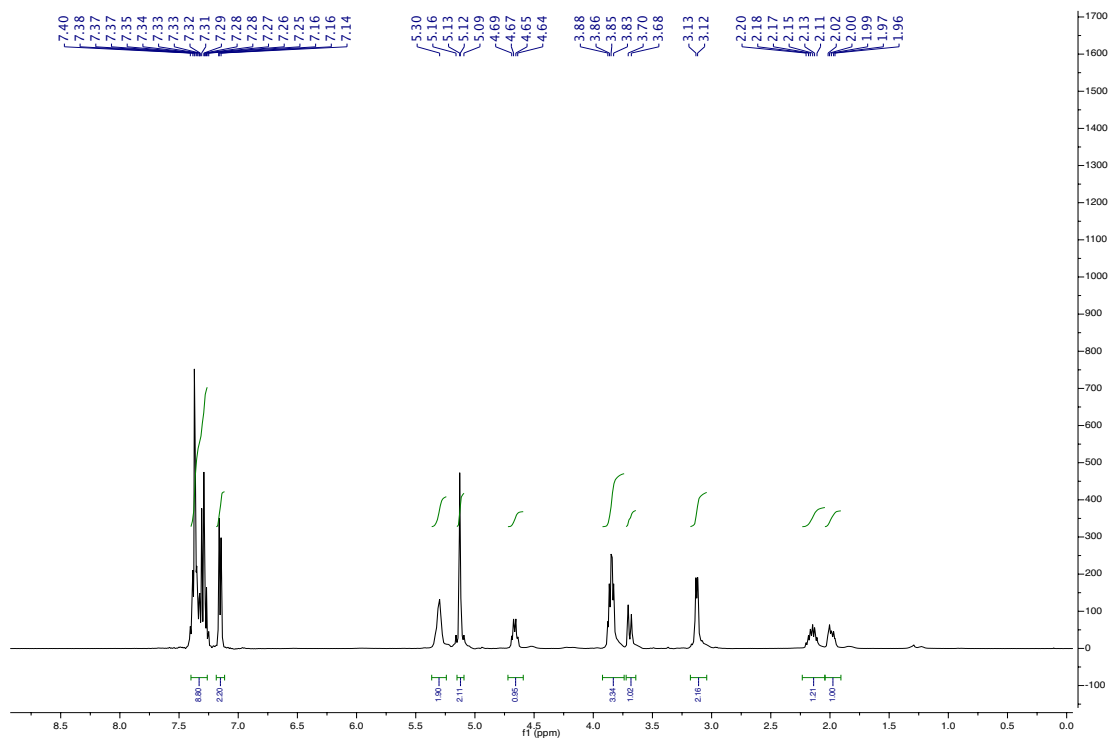


Fig. S6 NMR data of compound 6.

4.2 Dynamic light scattering

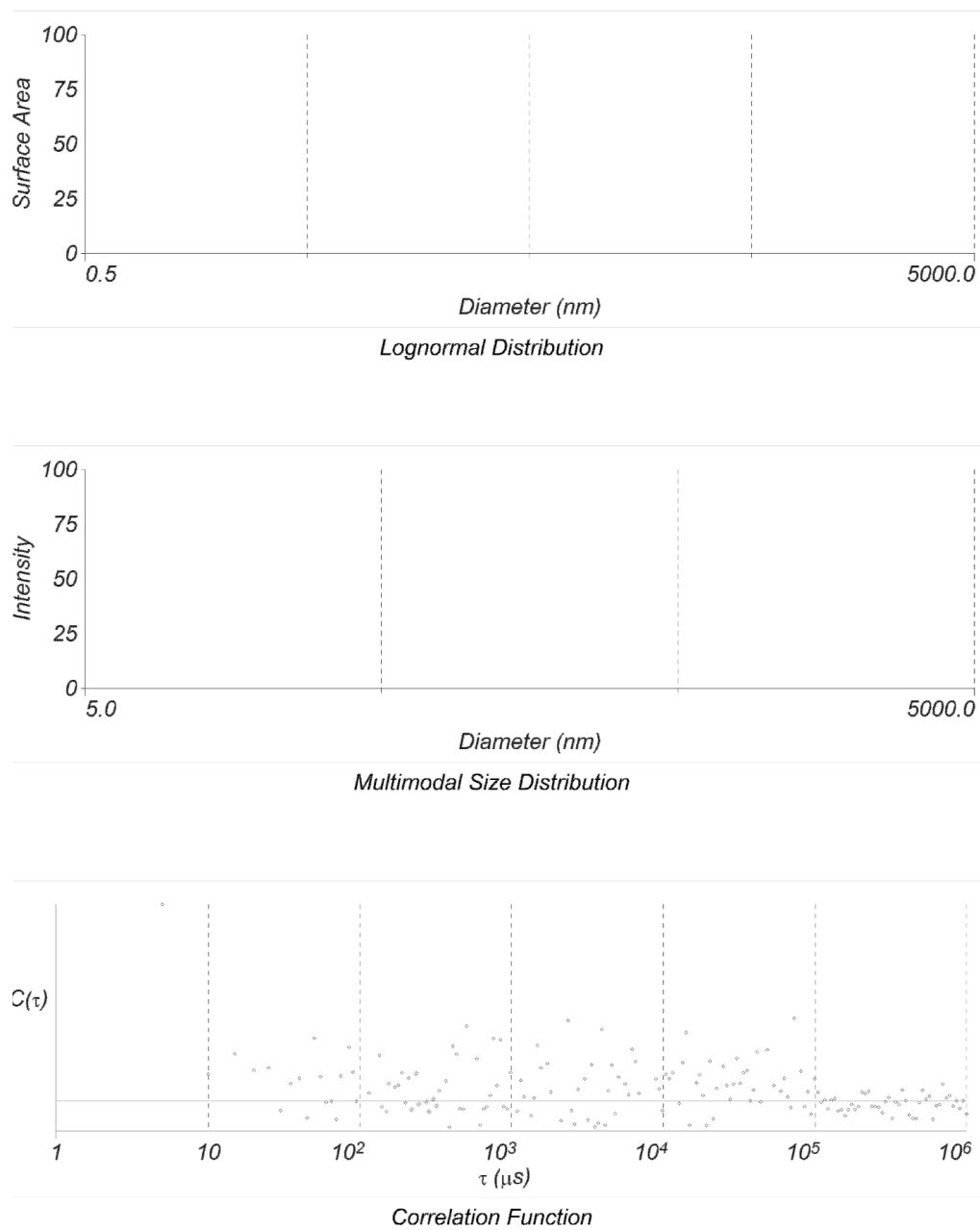


Fig. S7 DLS data of compound **3** at concentration of 50 μM.

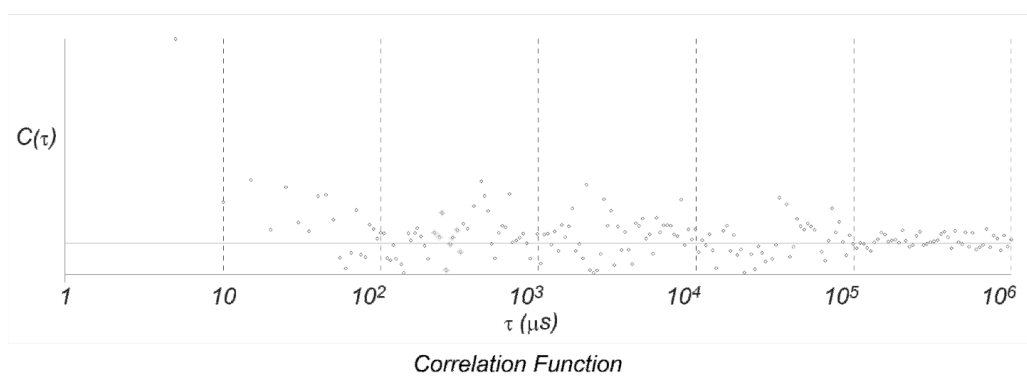
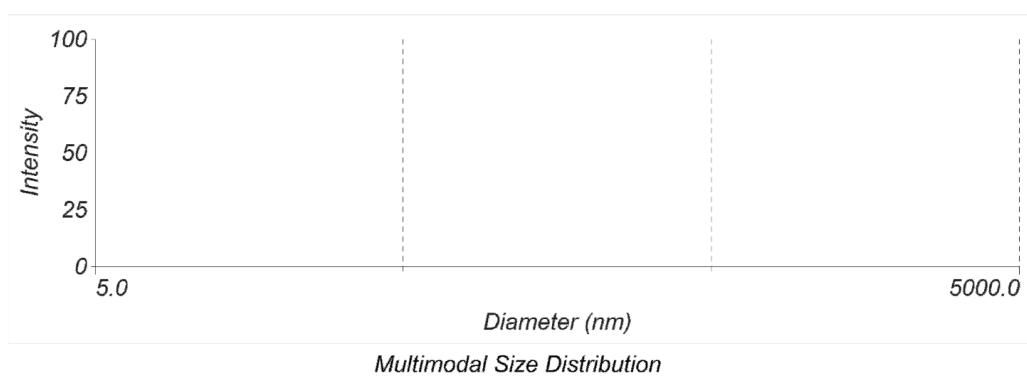
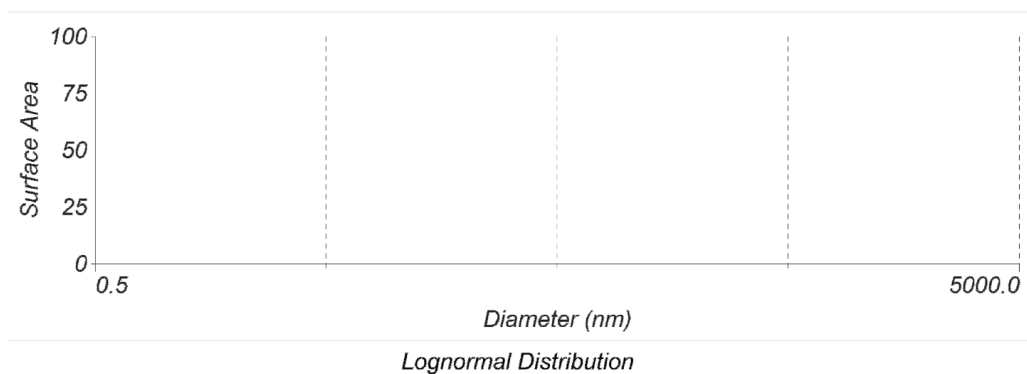
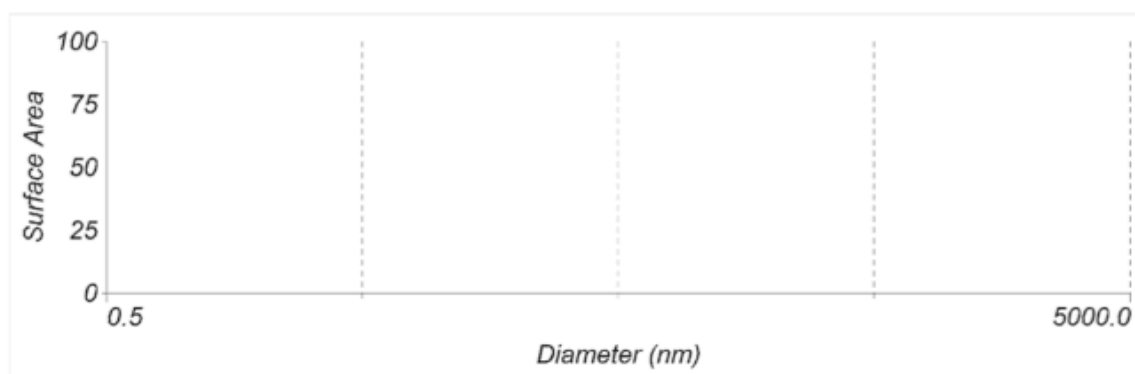
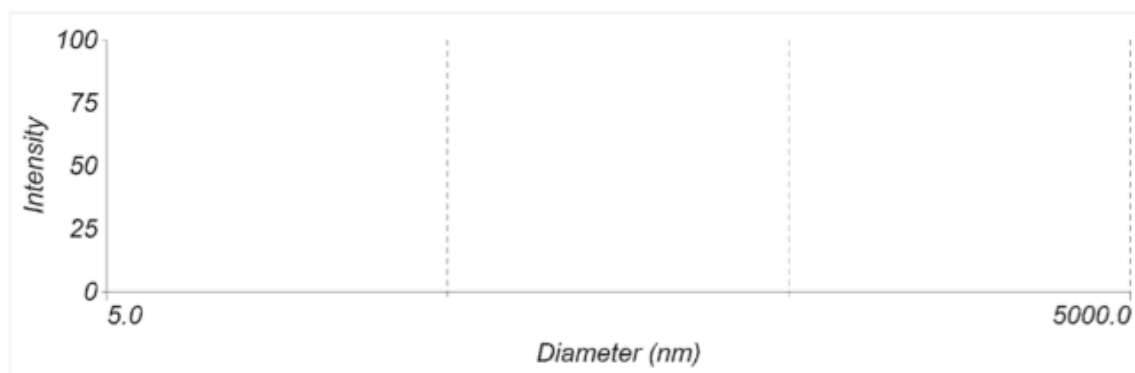


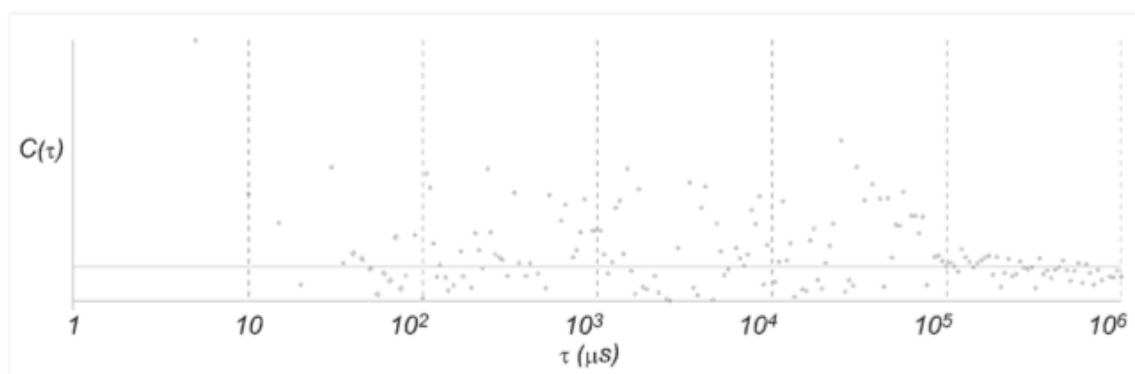
Fig. S8 DLS data of compound **4** at concentration of 100 μM .



Lognormal Distribution



Multimodal Size Distribution



Correlation Function

Fig. S9 DLS data of compound **5** at concentration of 100 μM .

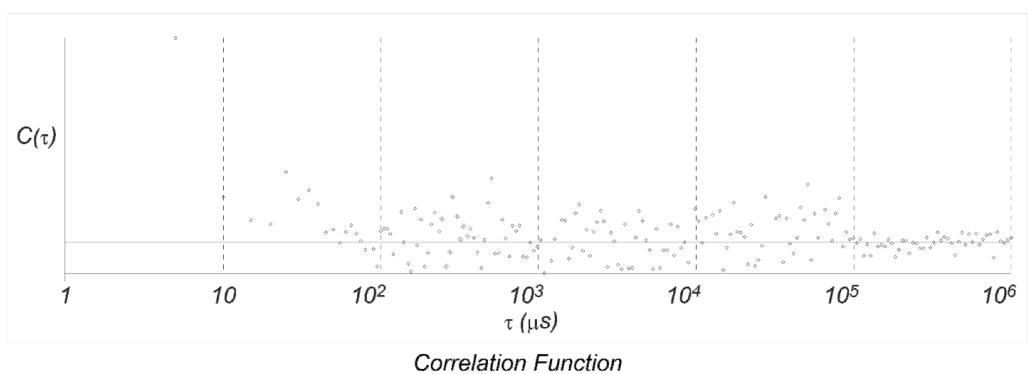
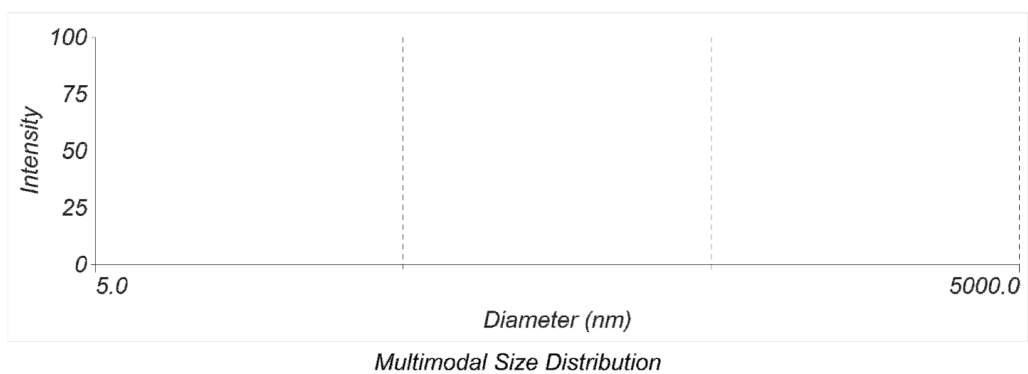
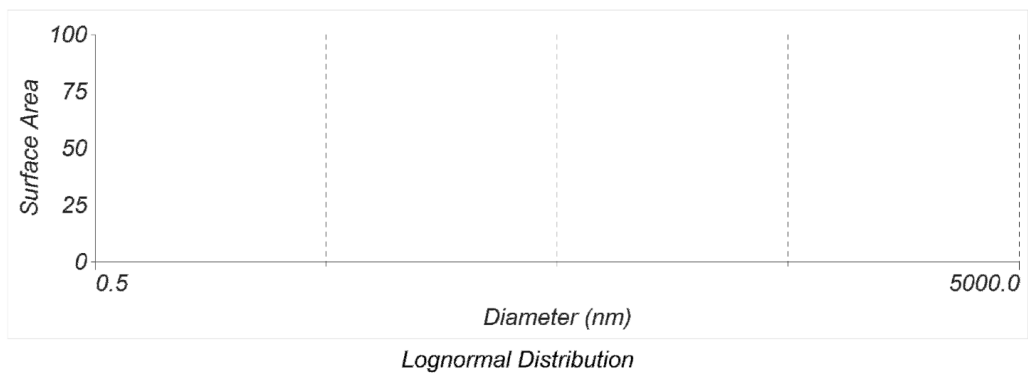


Fig. S10 DLS data of compound **6** at concentration of 100 μM .

4.3 Predicted affinity

Table S3. Predicted affinities (*pAffinity*) with Gaussian process models for compounds **1-6** and Mahalanobis distance (MD) to the background distribution.

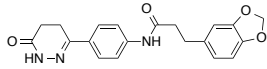
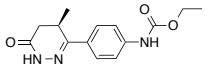
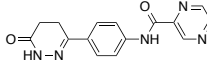
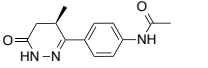
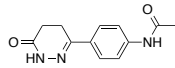
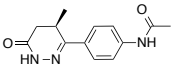
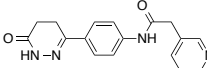
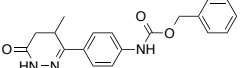
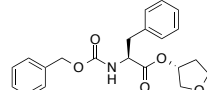
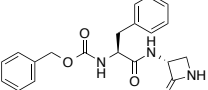
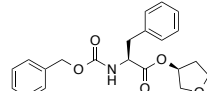
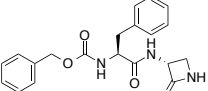
Compound	Target	<i>pAffinity</i>	MD
1	PDE3B	6.6	2.5
2	PDE3B	6.0	1.4
3	PDE3B	6.1	1.7
4	PDE3B	6.6	2.6
5	HIV-1 protease	5.8	4.5
6	HIV-1 protease	5.8	4.5

Table S4. PDE panel *pAffinity* and screening assay results for compound **4** at 50 μM ($n = 2$).

Target	<i>pAffinity</i>	% inhibition		
		1 st	2 nd	Mean
PDE2A1	3.7	9	6	8
PDE3A	6.1	95	77	86
PDE3B	6.6	95	89	92
PDE4A1A	5.6	2	7	5
PDE4B1	5.2	-2	1	-1
PDE7A	4.2	1	-8	-4
PDE10A2	4.8	65	52	59
PDE11A4	4.4	30	6	18

Controls – PDE2A1: EHNA ($IC_{50} = 1.6 \mu\text{M}$, *Hill* slope = -1.0); PDE3A: milrinone ($IC_{50} = 0.35 \mu\text{M}$, *Hill* slope = -1.1); PDE3B: milrinone ($IC_{50} = 0.67 \mu\text{M}$, *Hill* slope = -0.8); PDE4A1A: rolipram ($EC_{50} = 0.16 \mu\text{M}$, *Hill* slope = -1.0); PDE4A1B: rolipram ($EC_{50} = 0.087 \mu\text{M}$, *Hill* slope = -0.7); PDE7A: BRL 50481 ($EC_{50} = 0.66 \mu\text{M}$, *Hill* slope = -1.4); PDE10A2: papaverine ($IC_{50} = 0.092 \mu\text{M}$, *Hill* slope = -1.1); PDE11A4: dipyridamole ($IC_{50} = 0.87 \mu\text{M}$, *Hill* slope = -1.1).

Table S5. Nearest neighbors from the ChEMBL data set.

De novo designed entities		Nearest neighbours			
Cpd.	Structure	CHEMBL ID	Structure	IC₅₀ / μM	T_c^a
1		129691		0.0085 ⁹	0.31
2		340785		0.037 ⁹	0.36
3		340785		0.037 ⁹	0.58
4		129692		0.001 ⁹	0.36
5		281518		37.4 ¹⁰	0.50
6		281518		37.4 ¹⁰	0.50

^a Tanimoto coefficient (T_c) calculated with Morgan substructure fingerprints, *radius* 2; *nbit* = 2048; *pathlength* = 1-7.

4.4 Targets predicted with SEA and SPiDER for compounds 1-6

Table S6. SEA predictions for compound 1.

	Target	E-Value
1	Epstein-Barr nuclear antigen 1	3.54e-6
2	PDE3B	4.88e-5
3	PDE3A	1.07e-4
4	Caspase-2	4.80e-4
5	Histidinol dehydrogenase	1.60e-3
6	Histidinol dehydrogenase	3.11e-3
7	Histidinol dehydrogenase	3.11e-3
8	PDE3B	3.15e-3
9	PDE3B	4.33e-3
10	Caspase-2	8.45e-3

Table S7. SEA predictions for compound **2**.

	Target	E-Value
1	PDE3B	5.08e-8
2	PDE3A	1.47e-7
3	PDE3B	1.89e-6
4	PDE3B	2.25e-5
5	PDE3B	5.43e-4
6	PDE3A	1.50e-3
7	Interleukin-1 receptor associated kinase 4	5.51e-3
8	PDE3A	9.35e-2
9	PDE3B	2.00e-1
10	Sodium channel protein type X alpha unit	2.17e-1

Table S8. SEA predictions for compound **3**.

	Target	E-Value
1	PDE3B	1.32e-13
2	PDE3A	7.92e-13
3	Cytochrome c oxidase subunit 2	1.03e-11
4	Cytochrome c oxidase subunit 2	1.03e-11
5	Cytochrome c oxidase subunit 2	1.03e-11
6	PDE3B	5.39e-11
7	PDE3B	1.18e-9
8	PDE3B	1.36e-7
9	PDE3A	6.18e-7
10	Cytochrome P450 1A2	1.07e-6

Table S9. SEA predictions for compound **4**.

	Target	E-Value
1	Carbonic anhydrase VA	2.38e-12
2	Carbonic anhydrase VB	2.14e-11
3	Neuronal acetylcholine receptor protein alpha 7 subunit	1.97e-10
4	Neuronal acetylcholine receptor protein alpha 7 subunit	2.29e-10
5	Neuronal acetylcholine receptor protein alpha 7 subunit	7.06e-10
6	Neuronal acetylcholine receptor protein alpha 7 subunit	3.71e-9
7	Serine/Threonine-protein kinase mTOR	4.20e-9
8	Serine/Threonine-protein kinase mTOR	4.31e-8
9	PDE3B	5.39e-8
10	Poly [ADP-ribose] polymerase 2	1.39e-7

Table S10. SEA predictions for compounds **5** and **6**.

	Target	E-Value
1	Calpain 2	1.71e-158
2	Calpain 2	2.57e-157
3	Calpain 2	5.71e-144
4	Calpain 2	1.22e-134
5	Calpain 1	1.71e-133
6	Calpain 2	7.42e-132
7	Calpain 1	2.20e-128
8	Calpain 1	1.17e-120
9	Calpain 1	3.33e-120
10	Calpain 1	1.02e-113
13	HIV-1 protease	3-00e-96
31	Cathepsin L	8.96e-73

Table S11. SPiDER predictions for compound 1.

	Target	<i>p</i> value
1	Growth hormone releasing peptide receptor	0.003
2	Sodium channel	0.004
3	Cyclooxygenase	0.004
4	Nitric oxide synthase	0.004
5	Orexin receptor	0.005
6	Ionotropic glutamate receptor	0.005
7	Cystein proteases	0.005
8	Metabotropic glutamate receptor	0.006
9	Polymerase	0.006
10	Melanin concentrating hormone receptor	0.007
17	PDE	0.011

Table S12. SPiDER predictions for compound 2.

	Target	<i>p</i> value
1	Hypoxia-inducible factor prolyl hydroxylase	0.001
2	Aryl hydrocarbon receptor	0.003
3	Metabotropic glutamate receptor	0.004
4	Cyclooxygenase	0.004
5	RNA polymerase	0.004
6	Nitric oxide synthase	0.005
7	Polymerase	0.006
8	Nicotinic acetylcholine receptor	0.007
9	Deaminase	0.009
10	Histamine receptor	0.010
16	PDE	0.017

Table S13. SPiDER predictions for compound **3**.

	Target	<i>p</i> value
1	Metabotropic glutamate receptor	0.003
2	Tyrosine kinase	0.007
3	Aldose reductase	0.009
4	Phospholipase	0.010
5	PDE	0.014
6	Androgen receptor	0.019
7	DNA polymerase	0.023
8	Tumor necrosis factor alpha	0.025
9	Potassium channel	0.026
10	Adenosine receptor	0.026

Table S14. SPiDER predictions for compound **4**.

	Target	<i>p</i> value
1	Hypoxia-inducible factor prolyl hydroxylase	0.001
2	Metabotropic glutamate receptor	0.002
3	Aryl hydroxycarbon receptor	0.003
4	RNA polymerase	0.003
5	Histamine receptor	0.004
6	Nicotinic acetylcholine receptor	0.005
7	Cyclooxygenase	0.006
8	Cysteine protease	0.008
9	Polymerase	0.008
10	Deaminase	0.010
16	PDE	0.012

Table S15. SPiDER predictions for compounds **4**.

	Target	<i>p</i> value
1	Hypoxia-inducible factor prolyl hydroxylase	0.001
2	Metabotropic glutamate receptor	0.002
3	Aryl hydroxycarbon receptor	0.003
4	RNA polymerase	0.003
5	Histamine receptor	0.004
6	Nicotinic acetylcholine receptor	0.005
7	Cyclooxygenase	0.006
8	Cysteine protease	0.008
9	Polymerase	0.008
10	Deaminase	0.010
16	PDE	0.012

Table S16. SPiDER predictions for compounds **5** and **6**.

	Target	<i>p</i> value
1	Orexin receptor	0.002
2	Calcium channel	0.002
3	Dihydroorotate dehydrogenase	0.002
4	Sodium neurotransmitter symporter	0.004
5	Monoamine oxidase	0.006
6	Cysteine protease	0.006
7	Serine protease	0.007
8	Cyclooxygenase	0.008
9	Aspartic protease	0.009
10	Sodium channel	0.011
16	PDE	0.016

4.5 Biochemical data

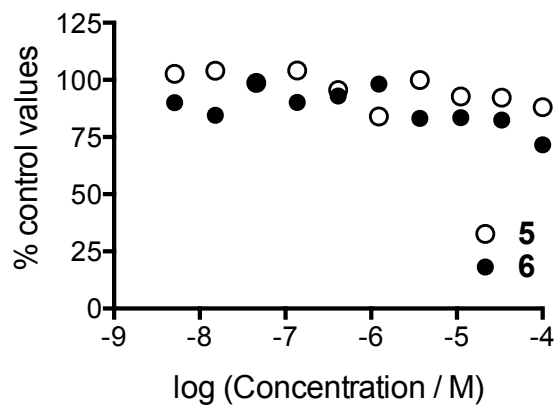


Fig. S11 Inhibition of Cathepsin S by compounds 5-6 ($n = 1$).

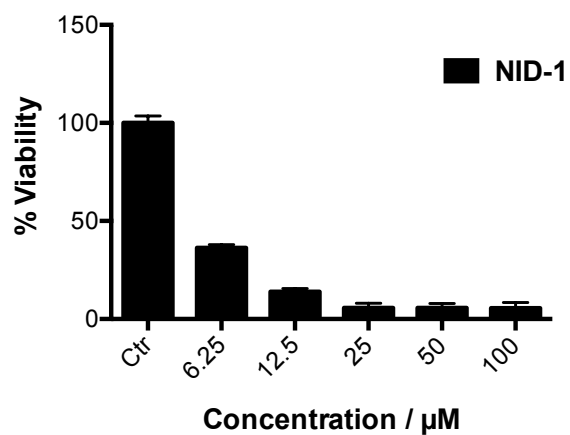


Fig. S12 MCF-7 (breast cancer cell line) viability upon 24 hour incubation with NID-1 at different concentrations ($n = 3$).

5. References

1. M. Hartenfeller, S. Renner and E. Jacoby, "Reaction-Driven De Novo Design: a Keystone for Automated Design of Target Family-Oriented Libraries" in *De Novo Molecular Design*, G. Schneider (Ed.), Wiley VCH, Weinheim (2013), pp. 245-266.
2. M. Hartenfeller, H. Zettl, M. Walter, M. Rupp, F. Reisen, E. Proschak, S. Weggen, H. Stark and G. Schneider, *PLoS Comput. Biol.*, 2012, **8**, e1002380.
3. M. Rupp and G. Schneider, *Mol. Inf.*, 2010, **29**, 266-273.
4. M. Reutlinger, T. Rodrigues, P. Schneider and G. Schneider, *Angew. Chem. Int. Ed.*, 2014, **53**, 582-585.
5. M. Reutlinger, T. Rodrigues, P. Schneider and G. Schneider, *Angew. Chem. Int. Ed.*, 2014, **53**, 4244-4248.
6. M. Reutlinger, C. P. Koch, D. Reker, N. Todoroff, P. Schneider, T. Rodrigues and G. Schneider, *Mol. Inf.*, 2013, **32**, 133-138.
7. A. T. Bender and J. A. Beavo, *Pharmacol. Rev.*, 2006, **58**, 488-520.
8. O. Kepp, L. Galluzzi, M. Lipinski, J. Yuan and G. Kroemer, *Nat. Rev. Drug Discov.*, 2011, **10**, 221-237.
9. S. D. Edmondson, A. Mastracchio, J. He, C. C. Chung, M. J. Forrest, S. Hofsess, E. MacIntyre, J. Metzger, N. O'Connor, K. Patel, X. Tong, M. R. Tota, L. H. Van der Ploeg, J. P. Varnerin, M. H. Fisher, M. J. Wyvratt, A. E. Weber and E. R. Parmee, *Bioorg. Med. Chem. Lett.*, 2003, **13**, 3983-3987.
10. N. E. Zhou, D. Guo, G. Thomas, A. V. Reddy, J. Kaleta, E. Purisima, R. Menard, R. G. Micetich and R. Singh, *Bioorg. Med. Chem. Lett.*, 2003, **13**, 139-141.